APS physics

CHORUS

This is the accepted manuscript made available via CHORUS. The article has been published as:

Determination of the Ion Temperature in a High-Energy-Density Plasma Using the Stark Effect

Dror Alumot, Eyal Kroupp, Evgeny Stambulchik, Alexander Starobinets, Ingo Uschmann, and Yitzhak Maron

Phys. Rev. Lett. **122**, 095001 — Published 6 March 2019

DOI: 10.1103/PhysRevLett.122.095001

Determination of the ion temperature in a high-energy-density plasma using Stark effect

Dror Alumot,[1,*] Eyal Kroupp,[1] Evgeny Stambulchik,[1,†] Alexander Starobinets,[1] Ingo Uschmann,[2] and Yitzhak Maron[1]

[1] *Faculty of Physics, Weizmann Institute of Science, Rehovot 7610001, Israel*

[2] *Institut für Optik und Quantenelektronik, Friedrich-Schiller-Universität Jena, Max-Wien-Platz 1, D-07743 Jena, Germany*

(Dated: February 12, 2019)

We present experimental determination of the ion temperature in a neon-puff Z-pinch. The diagnostic method is based on the effect of ion coupling on the Stark lineshapes. It was found, in a profoundly explicit way, that at stagnation the ion thermal energy is small compared to the imploding-plasma kinetic energy, where most of the latter is converted to hydromotion. The method here described can be applied to other highly non-uniform and transient high-energy-density plasmas, where realization of the previous approach is unfeasible.

PACS numbers: 52.58.Lq, 52.70.La, 32.60.+i, 32.70.-n

Introduction – The conversion of the kinetic energy of accelerated plasmas to ion heating, resulting in radiation emission or in nuclear fusion, is of fundamental interest in the field of high-energy-density (HED) plasmas, and has general implications for laboratory and astrophysical plasma research [1–6]. Of particular importance is determination of the ion thermal energy, addressed here.

In a stationary plasma, the ion temperature is associated with the spread of the kinetic energy K_i per ion. The latter is manifested in the Doppler broadening of spectral lines emitted [7] or, in the case of fusion plasmas, in a respective spread of the energy spectra of neutrons and other products of the fusion reactions [8–11]. However, for plasmas formed in the process of implosions, that is, in Z-pinches and inertial confinement fusion (ICF) experiments, both thermal *and* hydrodynamic motions contribute to K_i. Therefore, the *apparent* ion Doppler pseudo "temperature" $T_i^D = \frac{2}{3}\langle K_i\rangle$ may be a significant overestimation of the *true* ion temperature T_i. Indeed, it was shown [12] that the ion temperature at stagnation—a culmination of the plasma implosion—may be an order of magnitude (!) lower than T_i^D [13], with the rest of the kinetic energy likely stored in an ultrasonic turbulence [14]. However, even smaller differences between T_i^D and T_i are crucial for the fusion processes, whose rates depend drastically on T_i, while the residual kinetic energy [15] (hydromotion) is irrelevant. Furthermore, in an imploding plasma the electron temperature T_e [16] cannot be assumed to represent T_i, either: the radial kinetic energy is first transferred to T_i and then to T_e. Thus, $T_e < T_i < T_i^D$ until fully thermalized (which happens at late times, irrelevant for ICF).

The great challenge of determining true T_i was solved in the previous study [12] by performing a detailed energy balance on a specific region of the plasma, relying on measuring the *entire history* of $\langle K_i\rangle$ and many other parameters of the plasma in this region *and* around it. However, such extensive diagnostics and analysis are rarely feasible. Contrary to that, here we present direct measurements of the ion temperature in a HED plasma that avoid the energy-balance complexities by using a different approach, only requiring *localized instantaneous* spectroscopic data. The underlying physical phenomenon is the ion-temperature dependence of the Stark profile of certain lines in moderately coupled plasmas.

We demonstrate this approach by measuring T_i at the stagnation phase of a neon-puff *Z*-pinch, where, similar to the ICF implosions, the $T_e < T_i < T_i^D$ inequality holds [12]. *Z*-pinch is a pulsed-current system widely used [17] for studying plasma implosions and for producing HED plasmas. In this system, an intense azimuthal magnetic field B_θ, induced by an axial current J_z, radially collapses a pre-configured load. The load, imploding under the $\vec{J}\times\vec{B}$ force, stagnates near the pinch axis, where a hot-and-dense plasma is formed for a few nanoseconds. The stagnation phase in similar z-pinch devices studied earlier [12, 13, 18] is characterized by electron density and temperature $\lesssim 10^{21}\,\mathrm{cm}^{-3}$ and $\sim$200 eV, respectively. These parameters are also typical for the measurements described here. Lineshapes of H- and He-like neon ions were used for the diagnostics.

Stark-broadening sensitivity to T_i – Stark line broadening is widely used for plasma diagnostics [19]. The Stark width depends strongly on the plasma density (typically, between $\propto N_e^{2/3}$ and $\propto N_e$); this is true for broadening due to plasma electrons and ions alike. Contrary to that, the temperature dependence is rather weak and sometimes non-monotonous. Furthermore, the electron and ion contributions may have opposite tendencies resulting in a nearly complete cancellation over a wide temperature range [20]. Consequently, the Stark diagnostics is typically perceived synonymous to the density diagnostics. However, if N_e and T_e are known with a sufficient precision independently of the lineshape measurements (e.g., using the Thomson scattering [21] or dielectronic satellite ratios [22]), then even the moderate Stark-width sensitivity to T_i can be used to infer the latter; this approach is used in the present study.

The first members of spectroscopic series of hydrogen-like ions are affected by ion dynamics ([23] and references therein) and, therefore, are sensitive to T_i [24]. However, in HED plasmas the shapes of these lines are often dominated by the Doppler or opacity effects [7]. On the other hand, for lines that originate from levels with sufficiently high principal quantum number n (for brevity, "high-n lines") the ion dynamics is typically of little importance [25, 26]. Indeed the method employed here is based on a different phenomenon.

The static Stark effect in a hydrogen-like atom is propor-

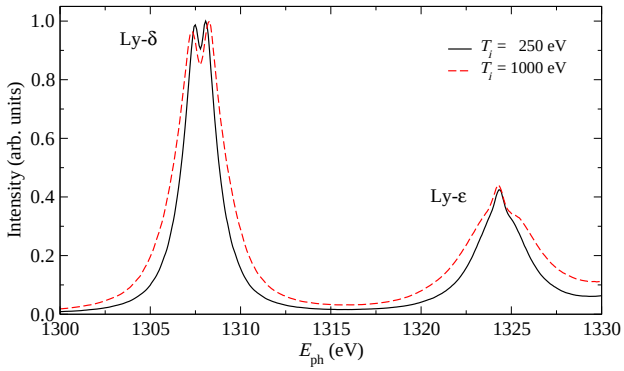

FIG. 1. Sensitivity of Stark broadening to the ion temperature. Results of computer simulations of the Ne X Lyman series in a neon plasma with $N_e = 10^{21}\,\mathrm{cm}^{-3}$ and $T_e = 250\,\mathrm{eV}$ are given (only shown is a spectral range containing Ly-δ and Ly-ε). The spectra are peak-normalized.

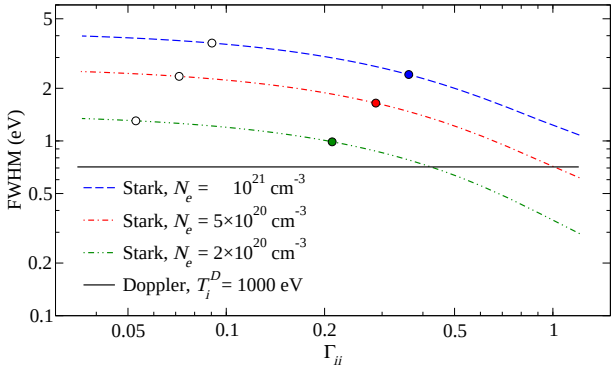

FIG. 2. Ne X Ly-δ Stark width as a function of Γ_{ii}, assuming three values of the electron density and a constant $T_e = 250\,\mathrm{eV}$. The filled and opaque circles correspond to $T_i = T_e = 250\,\mathrm{eV}$ and $T_i = T_i^D = 1000\,\mathrm{eV}$, respectively. Also shown is the Doppler broadening.

tional to the electric field F. In a plasma, the charged particles form a microfield distribution around the typical field value that depends on the density N_p and charge q_p of the plasma particles as $\propto |q_p| N_p^{2/3}$. This distribution is sufficient for evaluating the plasma broadening by the heavy plasma particles (ions) when their Stark effect can be described in the quasistatic approximation [19]. Furthermore, the electron broadening is usually smaller than that due to the ions, because of the dynamical nature of the electron perturbation [19] and the larger ion charge ($|q_i/e| > 1$). Thus, the broadening of these lines is mainly determined by the ion microfield distribution.

In an ideal plasma, the microfield distribution is a universal Holtsmark function [27] that is independent of temperature. However, Coulomb interactions between the particles modify [28] the Holtsmark distribution, due to the Debye screening and the repulsion between the ions and the positively charged radiators (which can be also expressed in terms of the ion radial distribution function $g(r)$ around the radiator), resulting in a decrease of the Stark broadening.

Figure 1 demonstrates this point, showing Ne X Ly-δ ($n = 5 \to n = 1$) and Ly-ε ($n = 6 \to n = 1$) Stark profiles calculated for fixed $N_e = 10^{21}\,\mathrm{cm}^{-3}$ and $T_e = 250\,\mathrm{eV}$ but assuming two different values of T_i. In the calculations, based on a variant [29] of the computer simulation modeling [30], all quantum states with $n \le 7$ were included [31]. As it is seen, the lower (equal to T_e) T_i results in noticeably narrower widths compared to those at the higher $T_i = 1000\,\mathrm{eV}$.

The Debye screening influences the ion fields at large distances ($r \gtrsim \lambda_{D,i}$, where $\lambda_{D,i}$ is the ion Debye length), while the Coulomb repulsion is only important at short distances ($r \lesssim r_{m,i}$, where $r_{m,i} = q_i^2/T_i$ is the classical distance of minimal approach). In a weakly non-ideal plasma the double inequality $r_{m,i} \ll r_i \ll \lambda_{D,i}$ holds, where $r_i = (4\pi N_i/3)^{-1/3}$ is a typical inter-ion distance; since the line width is mostly affected by microfields formed by ions at distances $\sim r_i$, the ion-temperature corrections in such a plasma are minor and the respective effect on the line broadening is small. However, the more non-ideal the plasma is (characterized by the ion–ion coupling parameter $\Gamma_{ii} = q_i^2/(r_i T_i)$), the stronger the corrections become.

As an example, in Fig. 2 shown is the width of Ne X Ly-δ, calculated [32] as a function of Γ_{ii} for a few values of the electron density at a fixed electron temperature. Ly-ε displays similar features. It is seen that for each density, there is a range of Γ_{ii} where the dependence of the Stark width on it and hence, on the ion temperature can be used for determination of T_i: for too high T_i (weakly coupled plasma) the Stark broadening is not sensitive to T_i, and for low T_i the Stark contribution becomes comparable or even smaller than the Doppler width, especially for lower plasma densities.

Experimental setup – Our Z-pinch generator (60 kV, 500 kA peak current, 500 ns rise time) implodes a neon-puff load in a 9-mm anode–cathode gap. The gas is injected into the gap through an annular nozzle (the cathode) that produces the outer gas cylinder, and through an on-axis nozzle, that produces the inner jet. Stagnation on axis of 10-ns duration is reached in ~500 ns.

The x-ray output from the stagnating plasma is recorded by a $\gtrsim$ 700-eV-filtered photoconductive detector (PCD). The spectroscopic system includes three spherical crystals, recording the neon Ly-α satellites and the high-n Ly-δ and Ly-ε, respectively. Each spectrometer allows for imaging the spectra along the Z-pinch axis with a spatial resolution of $\lesssim 50\,\mu$m. Two singly-gated (~1 ns) intensified charge-coupled device (CCD) cameras record the spectra collected by the spectrometers. The Ly-α satellite spectra are recorded with a 2nd-order spherical KAP crystal, yielding resolving power of $\gtrsim$ 6700 with a Lorentzian-shaped spectral response. Combined with collisional-radiative (CR) modeling [33], the spectra provide the time-resolved electron density and the total (thermal and hydro) ion velocities at any z position [12, 13]. Ly-δ and Ly-ε are recorded independently using two spherical 4th-order mica crystals, yielding resolving powers $\gtrsim$ 5000 with a

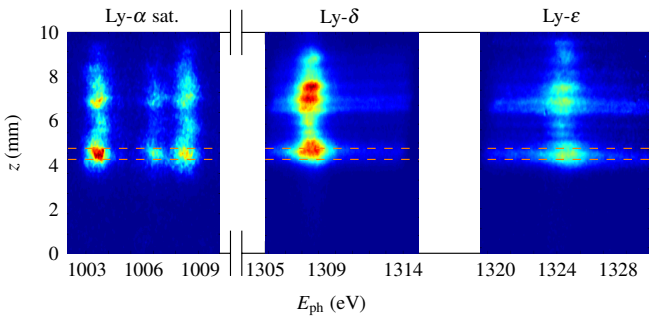

FIG. 3. Ly-α-satellites and high-n-line spectra recorded simultaneously at $t = 0$, axially resolved across the anode–cathode gap. The positions of the hot spots in all three spectra clearly match. The dashed lines highlight the slice from which the data are analyzed. The Ly-α and high-n spectra are normalized to the peak intensities of the Ly-α singlet satellite and Ly-δ, respectively.

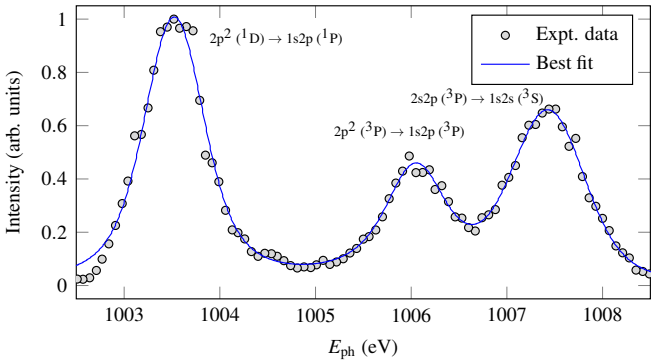

FIG. 4. Ne IX Ly-α satellite spectra: The experimental data are fit with three Voigt profiles. The Gaussian width of the singlet peak gives the total ion kinetic energy $T_i^D = 900 \pm 200\,\mathrm{eV}$, and the ratio between the integrated intensities of the two triplet groups gives the electron density $N_e = (6 \pm 1) \times 10^{20}\,\mathrm{cm}^{-3}$ using the CR modeling.

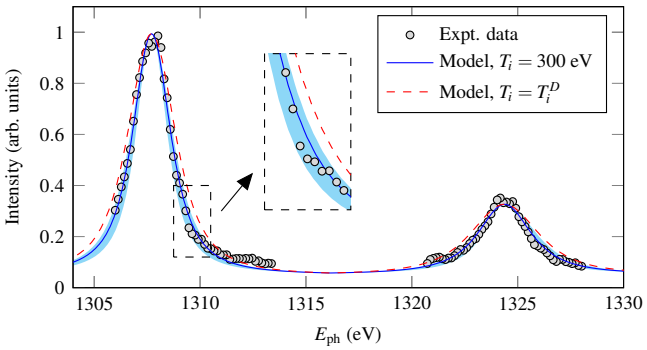

FIG. 5. The experimental high-n spectra are compared to lineshape modeling for two values of T_i assumed: 300 eV and T_i^D. $T_i^D = 900\,\mathrm{eV}$, $N_e = 6 \times 10^{20}\,\mathrm{cm}^{-3}$, and $T_e = 200\,\mathrm{eV}$ are assumed in both cases. The shaded area designates a spread of modeled spectra for T_i varying between 150 eV and 450 eV. An enlarged part of the graph is given in the inset.

Lorentzian-shaped instrumental broadening.

Two singly-gated multi-channel plate (MCP) detectors are used, one for the Ly-α satellite spectra, and the other for Ly-δ and Ly-ε. A high-voltage pulse generator is used to trigger both MCP detectors. With a delay correcting for the photon propagation, this allows for simultaneously recording all three spectra, imaged along z and integrated over the pinch chord. We note that even though a single high-n line is sufficient for application of the method, two such lines (Ly-δ and Ly-ε) were recorded to decrease the uncertainties.

See Supplemental Material at [URL] for more details on the experimental setup.

Results & Discussion – Typical spectra at the time of the peak PCD signal ($t = 0$) are shown in Fig. 3. In this example, analyzed are the z-averaged spectra from an axial slice $\Delta z = 0.5\,\mathrm{mm}$, centered at $z = 4.5\,\mathrm{mm}$ ($z = 0$ corresponds to the cathode surface).

The shapes of the singlet and two triplet-satellite groups are fit with Voigt profiles. The shape of the singlet Ly-α satellite provides, after deconvolution of the instrumental spectral response, the total Doppler broadening (the Stark broadening is negligible for these lines, the natural widths are small, and the opacities are very low for the present parameters), as has been described [12, 13]. For the example in Fig. 4 we obtain $T_i^D = 900 \pm 200\,\mathrm{eV}$. The triplet-to-singlet ratio of the integrated intensities of the satellite groups, together with CR modeling, is used to obtain the electron density in the plasma [12–14]. Accounting for the uncertainties in the experimental signals and in the atomic data used for the modeling, an effective [14] $N_e = (6 \pm 1) \times 10^{20}\,\mathrm{cm}^{-3}$ is obtained.

The spectra of Ly-δ and Ly-ε were modeled by convolving the calculated Stark lineshapes with the Doppler and instrumental broadenings. By varying T_i between zero and T_i^D, a best fit is obtained. T_e used in these calculations was determined to be $200 \pm 30\,\mathrm{eV}$ based on the continuum slope [18], and agrees with the values assumed in similar studies [12, 13]; the Stark lineshapes depend negligibly on T_e within this range. Results of the high-n lineshape analysis are presented in Fig. 5, demonstrating that the best fit is obtained for $T_i = 300 \pm 150\,\mathrm{eV}$, while assuming $T_i = T_i^D$ results in lineshapes that are far from fitting the data [34].

Spectral analysis was performed on multiple shots at various times throughout stagnation. The results are summarized in Table I. We observe that most of the kinetic energy of the ions is stored not in the thermal motion, but rather in a form of the hydrodynamic macro-motion, while the true ion temperature is, as a rule, close to the electron temperature. These findings are in qualitative agreement with the previous results [12] that were based on energy-balance considerations.

Since the measurements are radially integrated, the inferred values are weighted-average ones, with the local emissivity being the weighting function. Interestingly, at $t = 2\,\mathrm{ns}$ and 4 ns the inferred T_i is rather high, closer to T_i^D, which can be an indirect manifestation of the turbulent motion. Indeed, it was noted [14] that a plasma similar to the one studied here is likely to be slightly non-isothermal. In a non-isothermal

Shot #	t (ns)	N_e (10^{20} cm^{-3})	T_i^D (eV)	T_i (eV)
WIZ2149	−2.5	5.0 ± 1.0	1900 ± 400	400 ± 150
WIZ2119	−1.5	3.0 ± 0.5	1100 ± 300	300 ± 150
WIZ1684	−1.0	3.5 ± 0.5	1300 ± 300	350 ± 150
WIZ1715	0.0	6.0 ± 1.0	900 ± 200	300 ± 150
WIZ1676	2.0	2.5 ± 0.5	1000 ± 250	550 ± 250
WIZ1673	2.5	5.5 ± 1.0	600 ± 200	400 ± 150
WIZ2138	4.0	2.5 ± 0.5	600 ± 200	550 ± 200

TABLE I. The measured plasma parameters for various times throughout stagnation.

plasma, variations of the electron density and temperature are related through $T_e \propto N_e^{\gamma-1}$, where γ is the polytropic index ($\gamma = 1$ corresponds to isothermality). On the other hand, the intensity of the He-like satellites and that of H-like high-n lines depend differently on T_e, namely, the H-like line intensities rise with T_e significantly more strongly. Therefore, in the presence of turbulence-caused *positively correlated* fluctuations of N_e and T_e, the H-like Ly-δ and Ly-ε are on average emitted from higher-N_e regions than the He-like Ly-α satellites. Thus, N_e inferred from the Ly-α satellites is somewhat lower than the value required for calculating the Stark broadening of the H-like high-n lines. With N_e corrected, the Stark broadening would be larger, requiring a lower best-fit T_i to compensate (see Fig. 2). A deviation from the isothermality depends on the plasma density: the lower the density, the slower the thermal conduction [35]. Indeed, at $t = 2$ ns and 4 ns the density was rather low. Notably, the stagnated plasma in the much larger Z machine [36] has typical parameters [6] that ensure isothermality to a very high degree.

We emphasize that this is the first study where the ion temperature of a HED plasma is directly obtained from instantaneous localized measurements, without the necessity to obtain an entire history of the plasma parameters, and without relying on complex energy-balance argumentations. Thus, the approach described here may be considered for measurements in highly non-uniform and transient HED plasmas. The requirements for such measurements are (i) a moderate ion–ion coupling Γ_{ii}, (ii) the Stark broadening exceeding the Doppler one, and (iii) plasma with multiply-ionized ions. If, as is often the case, tracers are used for diagnostics, instead of Γ_{ii} one should use the radiator–ion coupling, $\Gamma_{ri} = q_r q_i/(r_i T_i)$ [29], where q_r is the charge of the radiator (tracer).

In Table II we list typical plasma parameters and suggested tracer lines for determining T_i in selected prominent experiments. There, the Stark-to-Doppler width ratios w_S/w_D were calculated assuming $T_i^D = T_i$, evidently underestimating the Doppler broadening. However, the ratios are $\gg 1$, so that there is always a safe margin to ensure the Stark effect dominates the total line width. For given plasma conditions, the ratio can be adjusted either by using a higher-n (a stronger Stark effect) or a lower-energy transition (thus, reducing the Doppler broadening), e.g., a Balmer ($n \to n = 2$) instead of a Lyman transition. Evidently, spectral lines of other charge states (e.g., He-like) can also be considered. Thus, the freedom of choosing the transition and the tracer species itself provides sufficient flexibility for employing the diagnostic method described here in a variety of major HED experiments.

Finally, we note that the uncertanties in the inferred T_i are in part due to uncertanties in the lineshape calculations; this study is not unique in this respect. The Spectral Line Shapes in Plasma code comparison workshops [39] represent a major effort for assessing the accuracy of lineshape models. However, to the best of our knowledge, no benchmark experiments exist at HED plasma conditions. Therefore, we believe this should urge the community to carry out such measurements.

Fruitful discussions with A. Fisher, and invaluable suggestions and reading the manuscript by O. L. Landen and M. B. Schneider are gratefully acknowledged. We thank P. Meiri for his skilled assistance, O. Wehrhan for preparing the mica crystals, and F. Schäfers and B. Marx for their help during the rocking curve measurements at BESSY-II. We are grateful to two anonymous referees for providing very valuable comments and suggestions. This work was supported in part by the Cornell Multi-University Center for High Energy-Density Science (USA), the Israel Science Foundation, and the Air Force Office of Scientific Research (USA).

* Present address: Applied Materials, Rehovot, Israel; Corresponding author: droralumot@gmail.com
† Corresponding author: evgeny.stambulchik@weizmann.ac.il

[1] B. A. Remington, R. P. Drake, and D. D. Ryutov, Rev. Mod. Phys. **78**, 755 (2006).
[2] M. Herrmann, Nature **506**, 302 (2014).
[3] S. A. Slutz, M. C. Herrmann, R. A. Vesey, A. B. Sefkow, D. B. Sinars, D. C. Rovang, K. J. Peterson, and M. E. Cuneo, Phys. Plasmas **17**, 056303 (2010); M. E. Cuneo, M. C. Herrmann, D. B. Sinars, S. A. Slutz, W. A. Stygar, R. A. Vesey, A. B. Sefkow, G. A. Rochau, G. A. Chandler, J. E. Bailey, J. L. Porter, R. D. McBride, D. C. Rovang, M. G. Mazarakis, E. P. Yu, D. C. Lamppa, K. J. Peterson, C. Nakhleh, S. B. Hansen, A. J. Lopez, M. E. Savage, C. A. Jennings, M. R. Martin, R. W. Lemke, B. W. Atherton, I. C. Smith, P. K. Rambo, M. Jones, M. R. Lopez, P. J. Christenson, M. A. Sweeney, B. Jones, L. A. McPherson, E. Harding, M. R. Gomez, P. F. Knapp, T. J. Awe, R. J. Leeper, C. L. Ruiz, G. W. Cooper, K. D. Hahn, J. McKenney, A. C. Owen, G. R. McKee, G. T. Leifeste, D. J. Ampleford, E. M. Waisman, A. Harvey-Thompson, R. J. Kaye, M. H. Hess, S. E. Rosenthal, and M. K. Matzen, IEEE Trans. Plasma Sci. **40**, 3222 (2012); M. R. Gomez, S. A. Slutz, A. B. Sefkow, D. B. Sinars, K. D. Hahn, S. B. Hansen, E. C. Harding, P. F. Knapp, P. F. Schmit, C. A. Jennings, T. J. Awe, M. Geissel, D. C. Rovang, G. A. Chandler, G. W. Cooper, M. E. Cuneo, A. J. Harvey-Thompson, M. C. Herrmann, M. H. Hess, O. Johns, D. C. Lamppa, M. R. Martin, R. D. McBride, K. J. Peterson, J. L. Porter, G. K. Robertson, G. A. Rochau, C. L. Ruiz, M. E. Savage, I. C. Smith, W. A. Stygar, and R. A. Vesey, Phys. Rev. Lett. **113**, 155003 (2014).
[4] J. E. Bailey, G. A. Chandler, S. A. Slutz, I. Golovkin, P. W. Lake, J. J. MacFarlane, R. C. Mancini, T. J. Burris-Mog, G. Cooper, R. J. Leeper, T. A. Mehlhorn, T. C. Moore, T. J. Nash, D. S. Nielsen, C. L. Ruiz, D. G. Schroen, and W. A.

Experiment	N_e (cm^{-3})	T_i (eV)	Plasma composition	$\lvert q_i/e\rvert$	Tracer line	Γ_{ri}	w_S/w_D
Radiating shock [5]	10^{22}	300	Plastic	3	Si Ly-γ	0.45	7
Capsule implosion [4]	2×10^{23}	3000	Plastic	3	Ar Ly-β	0.16	6
ICF hohlraum with dot tracers [37]	2×10^{21}	1000	Aluminum	13	Al Balmer-β	0.21	10
ICF gold bubble [38]	2×10^{21}	1000	Gold	50	Na Ly-ε	0.40	5

TABLE II. Typical plasma parameters and a suggested tracer transition for the analysis in a few major experiments. Also given are the radiator–ion-perturber coupling Γ_{ri} and the ratio of the Stark to Doppler broadening w_S/w_D, with $T_i^D = T_i$ assumed for the latter.

Varnum, Phys. Rev. Lett. **92**, 085002 (2004).

[5] G. A. Rochau, J. E. Bailey, Y. Maron, G. A. Chandler, G. S. Dunham, D. V. Fisher, V. I. Fisher, R. W. Lemke, J. J. MacFarlane, K. J. Peterson, D. G. Schroen, S. A. Slutz, and E. Stambulchik, Phys. Rev. Lett. **100**, 125004 (2008).

[6] Y. Maron, A. Starobinets, V. I. Fisher, E. Kroupp, D. Osin, A. Fisher, C. Deeney, C. A. Coverdale, P. D. Lepell, E. P. Yu, C. Jennings, M. E. Cuneo, M. C. Herrmann, J. L. Porter, T. A. Mehlhorn, and J. P. Apruzese, Phys. Rev. Lett. **111**, 035001 (2013).

[7] H. R. Griem, *Principles of Plasma Spectroscopy* (Cambridge University Press, Cambridge, England, 1997).

[8] B. Appelbe and J. Chittenden, Plasma Phys. Control. Fusion **53**, 045002 (2011).

[9] M. Gatu Johnson, D. T. Casey, J. A. Frenje, C.-K. Li, F. H. Séguin, R. D. Petrasso, R. Ashabranner, R. Bionta, S. LePape, M. McKernan, A. Mackinnon, J. D. Kilkenny, J. Knauer, and T. C. Sangster, Phys. Plasmas **20**, 042707 (2013).

[10] T. J. Murphy, Phys. Plasmas **21**, 072701 (2014).

[11] B. K. Spears, D. H. Munro, S. Sepke, J. Caggiano, D. Clark, R. Hatarik, A. Kritcher, D. Sayre, C. Yeamans, J. Knauer, T. Hilsabeck, and J. Kilkenny, Phys. Plasmas **22**, 056317 (2015).

[12] E. Kroupp, D. Osin, A. Starobinets, V. Fisher, V. Bernshtam, L. Weingarten, Y. Maron, I. Uschmann, E. Förster, A. Fisher, M. E. Cuneo, C. Deeney, and J. L. Giuliani, Phys. Rev. Lett. **107**, 105001 (2011).

[13] E. Kroupp, D. Osin, A. Starobinets, V. Fisher, V. Bernshtam, Y. Maron, I. Uschmann, E. Förster, A. Fisher, and C. Deeney, Phys. Rev. Lett. **98**, 115001 (2007).

[14] E. Kroupp, E. Stambulchik, A. Starobinets, D. Osin, V. I. Fisher, D. Alumot, Y. Maron, S. Davidovits, N. J. Fisch, and A. Fruchtman, Phys. Rev. E **97**, 013202 (2018).

[15] A. L. Kritcher, R. Town, D. Bradley, D. Clark, B. Spears, O. Jones, S. Haan, P. T. Springer, J. Lindl, R. H. H. Scott, D. Callahan, M. J. Edwards, and O. L. Landen, Phys. Plasmas **21**, 042708 (2014).

[16] L. C. Jarrott, B. Bachmann, T. Ma, L. R. Benedetti, F. E. Field, E. P. Hartouni, R. Hatarik, N. Izumi, S. F. Khan, O. L. Landen, S. R. Nagel, R. Nora, A. Pak, J. L. Peterson, M. B. Schneider, P. T. Springer, and P. K. Patel, Phys. Rev. Lett. **121**, 085001 (2018).

[17] D. D. Ryutov, M. S. Derzon, and M. K. Matzen, Rev. Mod. Phys. **72**, 167 (2000).

[18] D. Alumot, *Determination of the Temperature and Density of Hot-Dense Plasma by Measuring the X-Ray Continuum Spectra*, Master's thesis, Weizmann Institute of Science, Rehovot, Israel (2007).

[19] H. R. Griem, *Spectral Line Broadening by Plasmas* (Academic Press, New York, 1974).

[20] E. Stambulchik and A. V. Demura, J. Phys. B: At. Mol. Opt. Phys. **49**, 035701 (2016).

[21] S. Glenzer and R. Redmer, Rev. Mod. Phys. **81**, 1625 (2009).

[22] J. F. Seely, Phys. Rev. Lett. **42**, 1606 (1979).

[23] S. Ferri, A. Calisti, C. Mossé, J. Rosato, B. Talin, S. Alexiou, M. A. Gigosos, M. Á. González, D. González-Herrero, N. Lara, T. Gomez, C. A. Iglesias, S. Lorenzen, R. C. Mancini, and E. Stambulchik, Atoms **2**, 299 (2014).

[24] M. A. Gigosos, M. Á. González, and V. Cardeñoso, Spectrochim. Acta Part B **58**, 1489 (2003).

[25] E. Stambulchik, S. Alexiou, H. R. Griem, and P. C. Kepple, Phys. Rev. E **75**, 016401 (2007).

[26] S. Alexiou, E. Stambulchik, T. Gomez, and M. Koubiti, Atoms **6**, 13 (2018).

[27] J. Holtsmark, Ann. Phys. (Leipzig) **58**, 577 (1919).

[28] A. V. Demura, International Journal of Spectroscopy **2010**, 671073 (2010).

[29] E. Stambulchik and Y. Maron, J. Quant. Spectr. Rad. Transfer **99**, 730 (2006).

[30] E. Stambulchik and Y. Maron, High Energy Density Phys. **6**, 9 (2010).

[31] The interactions between the states with different n's result in a slight asymmetry of the lineshapes. In addition, the "blue" wing of Ly-ε is affected by blending with the "red" wing of the Ly-ζ line ($n = 7 \to n = 1$, not shown in Fig. 1).

[32] E. Stambulchik and Y. Maron, JINST **6**, P10009 (2011).

[33] Yu. V. Ralchenko and Y. Maron, J. Quant. Spectr. Rad. Transfer **71**, 609 (2001).

[34] In Supplemental Material [URL] we discuss accuracy of the lineshape modeling, referring to studies [40–46].

[35] Ya. B. Zeldovich and Yu. Raizer, *Physics of shock waves and high-temperature hydrodynamic phenomena* (Academic Press, New York, 1967).

[36] B. Jones, C. Deeney, C. Coverdale, P. LePell, J. McKenney, J. Apruzese, J. Thornhill, K. Whitney, R. Clark, A. Velikovich, J. Davis, Y. Maron, V. Kantsyrev, A. Safronova, and V. Oreshkin, J. Quant. Spectr. Rad. Transfer **99**, 341 (2006).

[37] M. A. Barrios, S. P. Regan, L. J. Suter, S. Glenn, L. R. Benedetti, D. K. Bradley, G. W. Collins, R. Epstein, B. A. Hammel, G. A. Kyrala, N. Izumi, T. Ma, H. Scott, and V. A. Smalyuk, Phys. Plasmas **20**, 072706 (2013); W. A. Farmer, O. S. Jones, M. A. Barrios, D. J. Strozzi, J. M. Koning, G. D. Kerbel, D. E. Hinkel, J. D. Moody, L. J. Suter, D. A. Liedahl, N. Lemos, D. C. Eder, R. L. Kauffman, O. L. Landen, A. S. Moore, and M. B. Schneider, Plasma Phys. Control. Fusion **60**, 044009 (2018).

[38] M. B. Schneider, S. A. MacLaren, K. Widmann, N. B. Meezan, J. H. Hammer, B. E. Yoxall, P. M. Bell, D. K. Bradley, D. A. Callahan, M. J. Edwards, T. M. Guymer, D. E. Hinkel, W. W. Hsing, M. L. Kervin, O. L. Landen, J. D. Moody, A. S. Moore, N. E. Palmer, and A. T. Teruya, J. Phys.: Conf. Ser. **717**, 012049 (2016); H. Chen, N. Palmer, M. Dayton, A. Carpenter, M. B. Schneider, P. M. Bell, D. K. Bradley, L. D. Claus, L. Fang, T. Hilsabeck, M. Hohenberger, O. S. Jones, J. D. Kilkenny, M. W. Kimmel, G. Robertson, G. Rochau, M. O. Sanchez, J. W. Stahoviak, D. C. Trotter, and J. L. Porter, Rev.

Sci. Instrum. **87**, 11E203 (2016).
[39] "Spectral Line Shapes in Plasmas workshops," http://plasma-gate.weizmann.ac.il/slsp/.
[40] J. M. J. van Leeuwen, J. Groeneveld, and J. de Boer, Physica **25**, 792 (1959).
[41] C. A. Iglesias, J. L. Lebowitz, and D. MacGowan, Phys. Rev. A **28**, 1667 (1983).
[42] A. Alastuey, C. A. Iglesias, J. L. Lebowitz, and D. Levesque, Phys. Rev. A **30**, 2537 (1984).
[43] B. Held and P. Pignolet, J. Physique **47**, 437 (1986).
[44] C. Iglesias, F. Rogers, R. Shepherd, A. Bar-Shalom, M. Murillo, D. Kilcrease, A. Calisti, and R. Lee, J. Quant. Spectr. Rad. Transfer **65**, 303 (2000).
[45] E. Stambulchik, D. V. Fisher, Y. Maron, H. R. Griem, and S. Alexiou, High Energy Density Phys. **3**, 272 (2007).
[46] E. Stambulchik and Y. Maron, Phys. Rev. E **87**, 053108 (2013).